Interactions during the chlorination of a copper–zinc alloy

G. De Micco [a,b,*], D.M. Pasquevich [a,c], A.E. Bohé [a,c,d]

[a] *Comisión Nacional de Energía Atómica (C.N.E.A.), Avenida Bustillo 9500, 8400 San Carlos de Bariloche, Argentina*
[b] *Universidad Nacional de Cuyo, Instituto Balseiro, Avenida Bustillo 9500, 8400 San Carlos de Bariloche, Argentina*
[c] *Consejo Nacional de Investigaciones Científicas y Técnicas (CONICET), Argentina*
[d] *Universidad Nacional del Comahue, Centro Regional Universitario Bariloche, 8400 San Carlos de Bariloche, Argentina*

Abstract

In this paper several aspects involved in the chlorination of a Zn 48% wt.–Cu alloy between 250 and 500 °C are investigated. The starting temperature for the chlorination of the alloy is determined, which is different from those of pure metals. Analysis of the chlorination thermogravimetric curves and reaction products reveal that there are interactions between reactants and products during the reaction, and that volatilization of $ZnCl_2$ is diminished during the alloy chlorination. Metallic copper is detected at intermediate stages of the chlorination, and this element, which is not present in the initial sample, appears during the chlorination reaction. An oxidation–reduction type reaction between copper chlorides and metallic zinc is proposed to explain the behaviour observed. The occurrence of this reaction at room temperature was confirmed in separate experiments. At the beginning of the reaction, formation of zinc oxichloride was detected that is being formed from the zinc oxide layer that covers the alloy surface. According to the results obtained, a reaction mechanism is presented for the alloy chlorination.
© 2008 Elsevier B.V. All rights reserved.

Keywords: Chlorination; Copper–zinc alloy; Thermogravimetry

1. Introduction

Copper and zinc are impurities of the AA6061 alloy used in fuel elements of nuclear research reactors. An aim of our institution is to diminish the amount of radioactive waste through the volatilization of the highest possible amount of aluminium accompanied by the smallest possible amount of radioactive impurities such as activated zinc. In previous studies, interferences in zinc volatilization were observed due to the presence of copper, which motivated the present work.

Metal chlorination reactions have been partially studied. Several works related with the chlorination of copper have been published [1–7]. While the first deal mainly with synthesis of copper(I) chloride by dry chlorination [1–3], the latter are focused on more basic aspects of the chemical heterogeneous reactions such as reaction mechanism and kinetics [4–7].

To the authors' best knowledge, no information is available regarding zinc dry chlorination reaction, with the only exception of the non-isothermal thermogravimetric (TG) curve for the

chlorination reaction that has been published by Tití-Manyaka and Iwasaki [8] in a work on chlorination of metals and oxides. This TG curve shows that the reaction starts at about 250 °C with a mass gain which corresponds to the formation of condensed zinc chlorides. After this, volatilization of chlorides is evidenced by a mass loss observed at about 600 °C. No studies regarding the kinetic or reaction mechanism were reported.

Besides its technological application for chloride synthesis [1,9,10], chlorination processes are proposed as a developing method for valuable metal recovery such as Co, Ni, V, W, Mo, Cr, Fe, Cu y Zn. For this reason, a number of studies involving chlorination of alloys or multi component systems were published [2,11,12].

Basic research in alloy chlorination [13–15] has shown that for Si–Ge, Mo–Re, Au–Pt, and Al–Cu alloys, the reactivity of the alloy is different from that of the pure constituents [13,15]. In addition, in the case of AlCu alloys, interactions between reaction products were reported during chlorination [15]. Similarly, interactions between reaction products and solid reactants were observed in the chlorination of multi-component systems [16].

Regarding the Cu–Zn system, a method for high-copper–zinc residue processing has been published by Chaudhary et al. [17]. The process developed involves leaching of the high-

---

* Corresponding author.
E-mail address: demiccog@cab.cnea.gov.ar (G. De Micco).

copper–zinc residues with concentrated hydrochloric acid, followed by electrodeposition of the solution obtained and dissolution of copper from the solid residue. As a result the separated metal chlorides are obtained. These kinds of processes related with zinc extraction or recovery of metals contained in ores and zinc industrial waste, involve interactions between copper and zinc and their compounds. Consequently, several studies appeared dealing with this topic. Ferry et al. [18] studied the electrolysis of zinc chloride with alkaline chlorides and the effect of other element [19–22].

No information related with dry chlorination of Cu–Zn alloys is available, which is why it is studied in this work. The presence of interactions during the reaction is revealed. These interactions are analyzed considering preferential oxidation, and oxidation–reduction reactions.

2. Experimental details

Commercial metals (99.9% purity) were used to prepare a Cu–Zn alloy with the following composition: Zn: 48 wt.%, Cu: 52 wt.%. This alloy was chosen for the study because the relative amount of each element ensures that the detection of reaction products and intermediate species is feasible by the different techniques available. Besides, we have considerable experience in our laboratory regarding its preparation and structural characterization. A powder of the alloy was prepared by mechanical abrasion with an electrical lathe (Black & Decker RT650). Thermal treatments at $300\,^{\circ}C$ for 2.5 h in air were performed to release possible residual tensions. The powder sample was well characterized by energy dispersive X-ray fluorescence (ED-XRF), scanning electron microscopy (SEM) and X-ray diffraction (XRD). The results are shown in Fig. 1.

As Fig. 1a shows, the powder consists of shavings of 150 μm average size. XRD patterns (Fig. 1b) show that the alloy is in beta phase. This phase has a composition range of Cu–(36.7–59.8)Zn (wt.%) [23].

The gases used were Cl_2 99.8% purity (Indupa, Argentina) and Ar 99.99% purity (AGA, Argentina). Isothermal and non-isothermal chlorination reactions were carried out with samples of 20 mg in a thermogravimetric analyzer (TGA). The equipment

as well as the methodology used to perform the chlorination were extensively described elsewhere [15].

3. Theoretical analysis

A preliminary theoretical analysis can be made taking into account the ΔG° values for all the feasible reactions which involve the elements contained in the system under study. In an ideal closed system, the final equilibrium composition will be determined only by the reaction having the lowest ΔG° value. However, in a closed system with multiple reactions like the one presented here, there are parallel reactions occurring simultaneously. This can lead to different intermediate products that may interact with the initial reactive species. Therefore, the equilibrium composition given by the reaction with the most negative ΔG° value may not always be attained, because the chemical reactions can reach pseudo-equilibriums that correspond to local minimums of ΔG°. This discrepancy is due to kinetical impedances which may include mass transfer, adsorption of different species, differences in the intrinsic rates of reactions, among others.

The TG analyzer is a flowing system. However, under certain circumstances the system may evolve following equilibrium predictions, and for this reason a thermodynamical analysis can give a first approximation. The expected behaviour can be obtained considering the Ellingahm diagram shown in Fig. 2 [24].

The ΔG° values for the chlorination of copper and zinc by mole of Cl_2 according to different reactions involving several species are shown in Fig. 2a. Copper has two stable chlorides, CuCl and $CuCl_2$, which correspond to the states of oxidation +1 and +2. Zinc only forms one stable chloride, $ZnCl_2$, according to its unique oxidation state +2. At high temperatures (about 1400 K) the presence of ZnCl(g) has been reported [25]. For this reason, ZnCl is also considered in the analysis. However, as evidenced in Fig. 2a, the ΔG° corresponding to the formation of ZnCl(g) is higher than that of $ZnCl_2$, which makes its occurrence very unlikely in the range for temperatures below $1000\,^{\circ}C$. Consequently, it will not be considered when analyzing the experimental results.
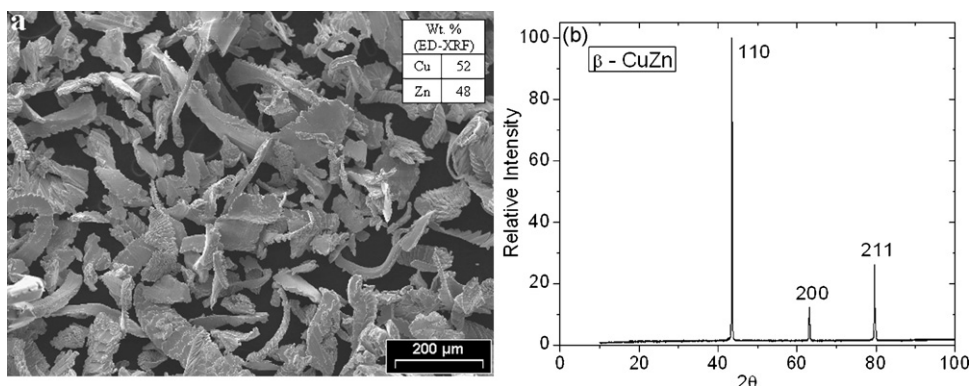

Fig. 1. Morphology, composition and structure of the initial sample. (a) SEM photograph of the Zn 48% wt.–Cu alloy powder and chemical composition obtained by ED-XRF. (b) XRD pattern of the initial sample.
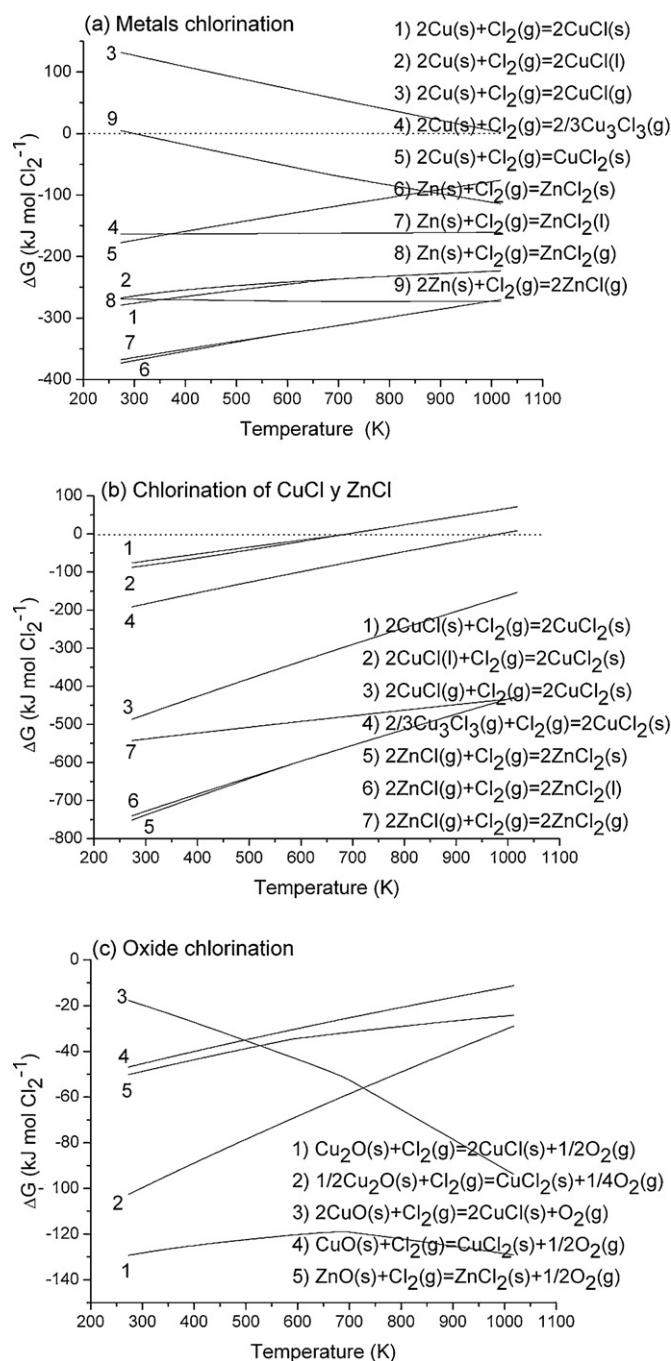
Fig. 2. Ellingham diagrams corresponding to (a) chlorination of metals, (b) chlorination of CuCl and ZnCl, (c) chlorination of oxides.

tial pressure of Cl_2, which is given by the incoming chlorine stream, will remain constant at 35.5 kPa. For this reason, the values of ΔG will be lower than the values of ΔG°, and even with a $\Delta G^\circ > 0$ a reaction could occur. The possible reactions are the ones listed in Fig. 2a.

In Fig. 2b the ΔG° values for the chlorination of CuCl and ZnCl(g) are presented. This could correspond to an advanced stage of the chlorination reaction where there are no more metallic elements. In this situation, the negative values of ΔG° indicate that ZnCl(g) will form $ZnCl_2$ in the first place, followed by formation of $CuCl_2$ from CuCl. Regarding the different chloride phases, Fig. 2a also shows that for temperatures below 1000 °C the stable chlorides are CuCl(s), CuCl(l) (above 425 °C), $ZnCl_2$(s) and $ZnCl_2$(l) (above 320 °C), and $CuCl_2$ which only exists in the solid state [4,24,26].

Finally, the oxide chlorination reactions are considered in Fig. 2c to analyze the expected reactivity of the metals. It is well known that when some metals such as aluminum, zirconium and refractory metals are put in contact with air, an oxide scale is formed [27] which protects the metals from further chemical attack. This is why, although these metals have negative ΔG° values for the chlorination reactions, they will not react when they are put in direct contact with chlorine until the conditions are appropriate for its penetration through the oxide film and the contact of the gas with the bulk metal is made. Chlorine can reach the base metal by chlorination of the protective oxide scale or by diffusion through grain boundaries or structural vacancies of the oxide film.

In the case of copper and zinc the ΔG° values for the oxidation reactions are negative for temperatures below 1000 °C [24]. Copper and zinc oxide layers do not have protective properties, as is well evidenced by the corrosion problems which affect copper devices or zinc plates under corrosive atmospheres. However, in a laboratory environment, where the atmospheric conditions are not favorable for the oxidation reaction, a thin oxide scale could still probably be formed on the metal surface. This oxide layer may have some influence in the metal reactivity during the chlorination reaction at the temperatures studied.

According to the ΔG° values for the reactions of copper and zinc oxides with chlorine, for temperatures below 1000 °C presented in Fig. 2c, both metal oxides will react. In the case of copper, it has two oxides with Cu_2O being the most reactive one. Therefore, taking into account thermodynamical data, none of these oxides would protect the metal towards chlorination. However, the starting temperatures for the chlorination could be determined by the kinetic rate of reaction of the oxides.

4. Results

4.1. Non-isothermal chlorination of Cu–Zn alloy

The initial reaction temperature which is associated with the system reactivity was determined by non-isothermal thermogravimetric measurements. The chlorination curves for the alloy
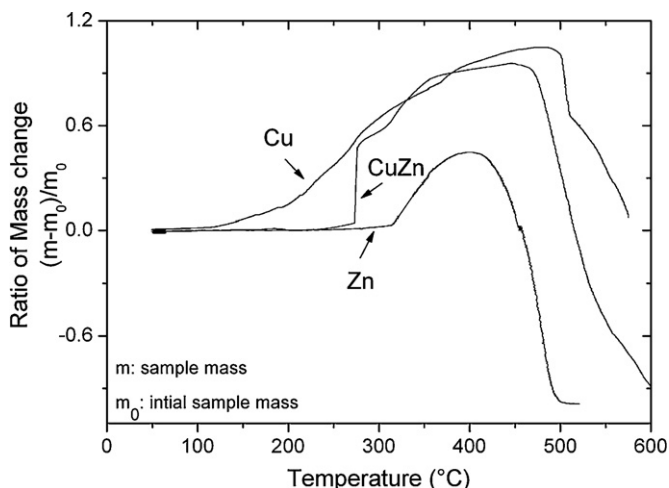
Among all the possible reactions, the formation of $ZnCl_2$(s,l) is the one that has the most negative ΔG°. Therefore, as long as there is still metallic zinc in the system, $ZnCl_2$(s,l) is the expected product according to equilibrium predictions for temperatures below 1000 °C. However, as mentioned before, other reactions having negative ΔG° values can occur due to local equilibriums. Moreover, the experimental set-up allows the continuous evacuation of gaseous reaction products (i.e. CuCl, Cu_3Cl_3, $ZnCl_2$ or ZnCl from reactions (3), (4), (8) and (9) Fig. 2a). Consequently, partial pressures of these species will tend to zero, whereas par-

Fig. 3. Non-isothermal TG curves for the chlorination of Cu, Zn y Zn 48% wt.–Cu alloy.

Fig. 4. Isothermal TG curve for the chlorination of Zn 48% wt.–Cu alloy between 250 and 500 °C.

together with the chlorination of the pure metals are shown in Fig. 3. Fig. 3 shows the ratio between the mass change and the initial mass of the sample as a function of temperature.

According to the selective oxidation phenomenon that takes place in several alloys, the less noble element is oxidized preferentially forming a continuous layer of oxide on the alloy surface. This happens, for example, in the case of copper alloyed with aluminium, silicon and beryllium [28]. For this reason, it is to be expected that the Cu–Zn alloy surface will be covered by a thin layer of zinc oxide. However, the scale formed on the alloy and that formed on the pure zinc surface will not necessarily have the same microstructure. This is in accordance with the differences observed in the chlorination starting temperatures of the alloy and pure zinc, considering that they are determined by chlorine diffusion across the oxide layer.

Fig. 3 shows that the starting temperature for the reaction of the alloy is in between those of the pure metals. Copper and zinc chlorination reactions start at about 100 and 270 °C, respectively. Meanwhile, the alloy reaction starts at 225 °C.

If chlorination of the oxide layer were the controlling phenomenon for the reaction starting temperature, both temperatures (for the chlorination of zinc and the alloy) should be the same, and would correspond to the starting temperature for the chlorination of zinc oxide: around 450 °C [29].

Fig. 3 also shows that the alloy chlorination reaction occurs with mass gain followed by mass loss above 450 °C. This is in accordance with the behaviours observed in pure metal chlorinations. For both metals an initial mass gain is observed due to the formation of condensed chlorides followed by a mass loss that indicates volatilization of the chlorides (and also decomposition in the case of copper [7]). Considering the ratio of the mass gain obtained in the chlorination of the pure metals and the alloy composition, the maximum ratio of mass gain for the alloy should be of 0.7. On the other hand, considering complete formation of $CuCl_2$ and $ZnCl_2$ the ratio of mass gain should be of 1.1. The ratio of mass gain obtained in the maximum of the chlorination TG curve was 0.95. This value indicates the forma-
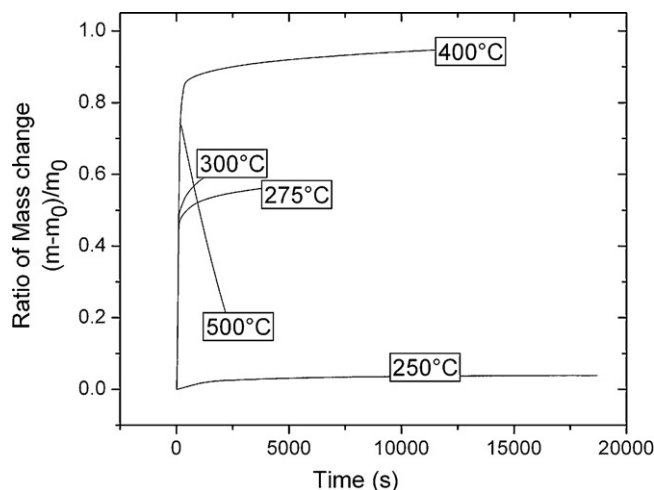
tion of larger amounts of condensed zinc chlorides during the chlorination of the alloy compared with pure zinc chlorination.

4.2. Isothermal chlorination of Cu–Zn alloy

4.2.1. Zinc retention

Isothermal chlorination reactions were carried out at different temperatures between 250 and 500 °C. The corresponding TG curves are shown in Fig. 4. The mass gains observed indicate the formation of condensed chlorides.

At 250 °C the low value of mass gain observed in the TG curve indicates that the reaction proceeds only to a very little extent. XRD analysis of the final sample reveals the presence of zinc oxichloride (Ref. Pat.: 45-0819; a, 5.86; b, 6.58 and c, 11.36 [30]) and alpha phase (α-Cu–Zn). This is a copper-rich phase, which is not present in the initial sample, and has a maximum content of zinc of 39 wt.% [23]. Regarding Zn_2OCl_2, this compound is being formed from the thin layer of zinc oxide that covers the alloy. The reaction interruption is attributed to this specie that forms a barrier which prevents further chlorination of the alloy.

The ratios of mass gain observed in the alloy chlorinations at higher temperatures indicate that there are interactions between copper and zinc that lead to the formation of larger amounts of condensed zinc chlorides. To show this, in Fig. 5 the TG curves at 300 and 400 °C are compared with simulated curves that were calculated considering the individual behaviour of each metal and the alloy composition as follows:

$$f_{Cu-Zn}^s(t) = x_{Cu} f_{Cu}^e(t) + x_{Zn} f_{Zn}^e(t) \tag{1}$$

$f_{Cu-Zn}^s(t)$: ratio between the mass change and the initial mass of the alloy as a function of time, simulated taking into account the chlorination reactions of Cu and Zn on their own.

$f_j^e(t)$: ratio between the mass change and the initial mass of metal j as a function of time, obtained experimentally form the chlorination of the corresponding metal. x_j: weight fraction of metal j in the alloy.
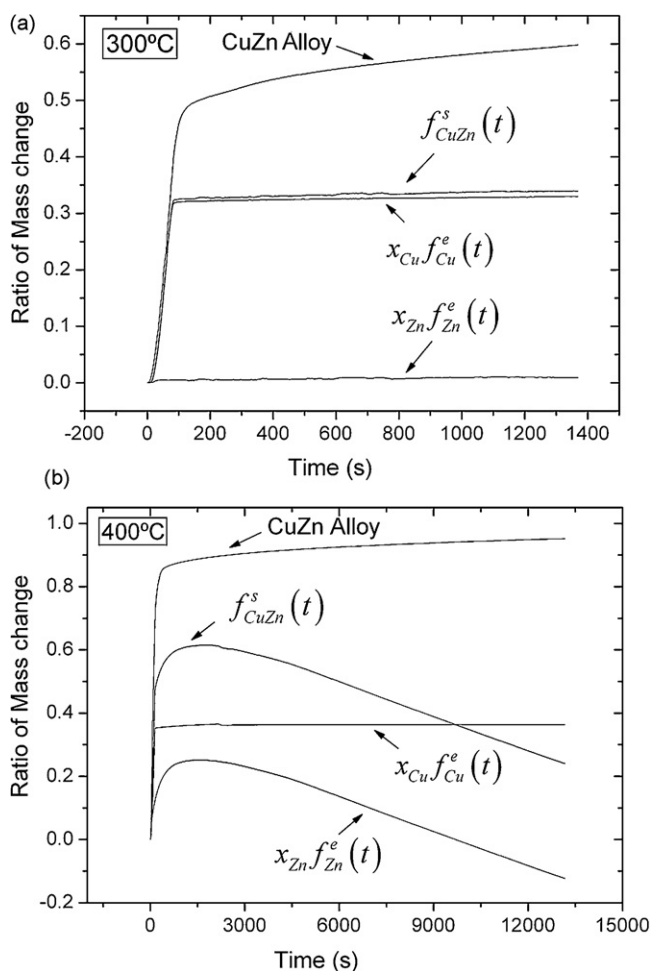
Fig. 5. Isothermal TG curves for the chlorination of Zn 48% wt.–Cu alloy at 300 and 400 °C, together with the metal chlorination curves, and the simulated curve considering the individual contributions of the metals.

Fig. 6. XRD pattern of the final sample from the chlorination of Zn 48% wt.–Cu alloy at 275 °C.

At 300 °C it can be seen that the mass gain obtained in the alloy chlorination is higher than the one expected for the chlorination of the pure metals in the alloy ratio. During the alloy chlorination a rapid mass gain is observed that reaches a value of 50% of the initial mass. Considering the individual metal behaviours a mass gain of only 32% of the initial mass would be achievable. The same happens at 400 °C, where the mass gain obtained in the alloy chlorination is 95% of the initial mass, while that expected considering the pure metals would be 60% of the initial mass. Moreover, during chlorination of pure zinc at 400 °C zinc chloride volatilization does occur. On the contrary, during alloy reaction, volatilization of ZnCl$_2$ was not detected as evidenced in the TG curve for the alloy chlorination which only shows mass gain. At this temperature, retention of zinc chlorides in the condensed phase occurs, although the vapour pressure (Eq. (2)) is high enough for its evaporation.

$$P^{vap}(kPa) = 3 10^{-8}T^3 - 6 10^{-5}T^2 + 0.0412T - 9.8997$$

$$673 < T(K) < 873 \tag{2}$$

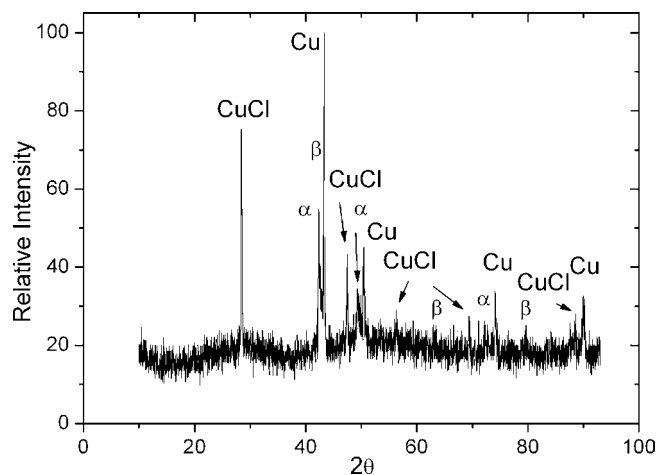### 4.2.2. Oxidation–reduction type interactions

Analysis of the reaction products at 275 and 300 °C by SEM and XRD reveals the presence of metallic copper. In Fig. 6 the XRD pattern corresponding to the sample chlorinated at 275 °C is shown. XRD analyses of the reaction products at 275 and 300 °C show that there is β-Cu–Zn (initial sample), a copper-rich phase α-Cu–Zn, CuCl and metallic copper. Zinc chloride is deliquescent, which is why it is difficult to detect this specie by XRD.

Fig. 7 belongs to the samples chlorinated at 275 and 300 °C analyzed by SEM. The presence of well-developed crystals can be observed, whose composition analyzed by EDS reveals that they correspond mainly to metallic copper. The presence of CuCl is not predicted by thermodynamic considerations below 400 °C where CuCl$_2$ is the most stable chloride (see Section 3). These results can be explained considering the electrochemical potentials of the different metal pairs (Table 1). According to Table 1 those species containing Cu^{+2} and Cu$^+$ will be reduced to copper by metallic zinc. For this reason, copper chlorides formed during the reaction would not remain unreacted as long as there is zinc in the sample. It is expected that during the reaction copper chlorides react with zinc leading to copper reduced species (Cu$^+$ and Cu).

To check the occurrence of these oxidation–reduction reactions between zinc and copper chlorides, samples were prepared consisting of powder of copper chlorides (CuCl$_2$ and CuCl) mixed with powder of Cu–Zn alloy. The mixtures were aged at room temperature for different time periods in argon atmosphere. Fig. 8a and b show XRD patterns obtained after 5 and 30 h of ageing. Appearance of metallic copper and dis-

Table 1
Electrochemical standard potentials of metal pairs for Cu and Zn species

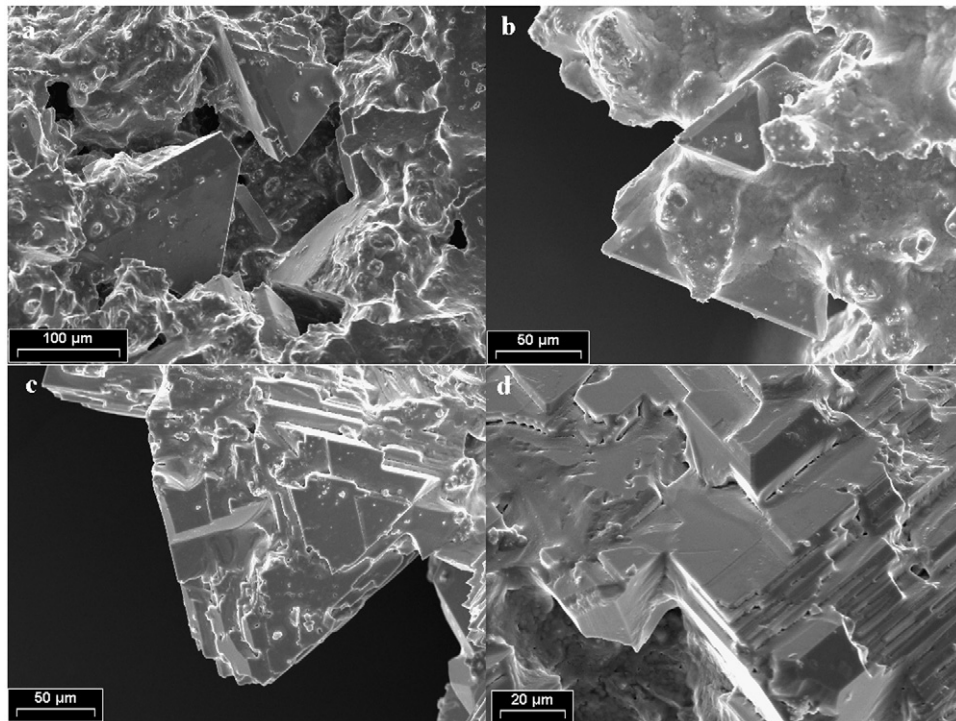| Electrochemical potential of metal pairs	$E°$, V (298.15 K, 101.325 kPa)
Cu^{2+}/Cu//Zn/Zn^{2+}	1.1037
Cu^{2+}/Cu$^+$//Zn/Zn^{2+}	0.9148
Cu$^+$/Cu//Zn/Zn^{2+}	1.2828

Fig. 7. (a) and (b) SEM photograph of the final sample from the chlorination at 275 °C, (c) and (d) SEM photograph of the final sample from the chlorination at 300 °C.

appearance of $CuCl_2$ were observed in all the aged samples. SEM and EDS analyses shown in Fig. 8c and d reveal the formation of well-defined copper crystals and the appearance of copper-rich zones. Consequently, the occurrence of the oxidation–reduction reactions was confirmed at room temperature. Therefore, during chlorination the kinetics of these reactions will be faster due to high temperature condition.
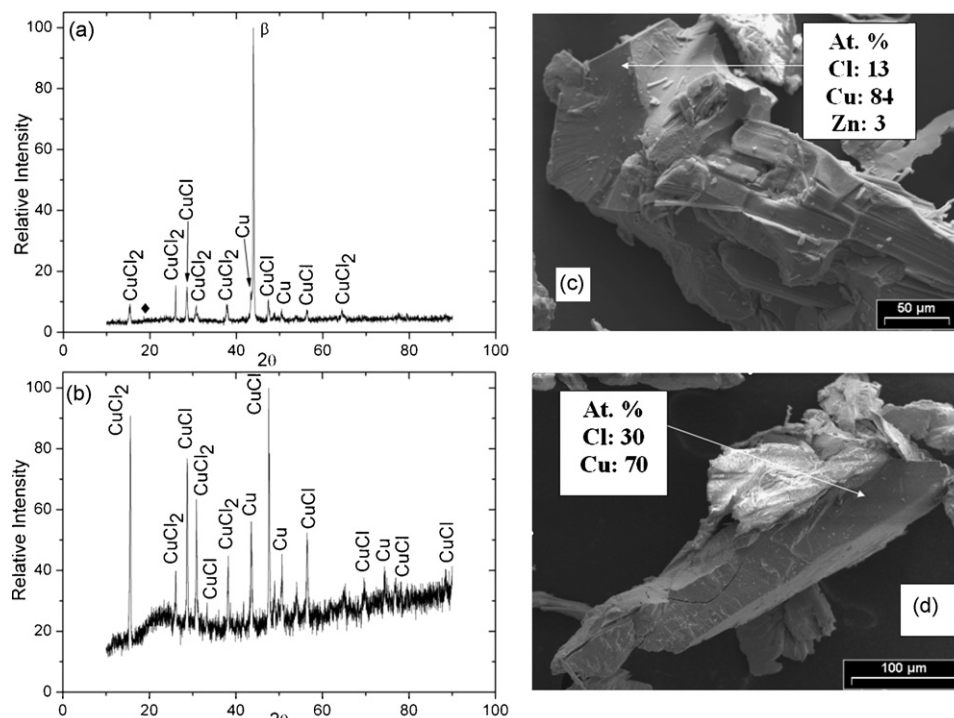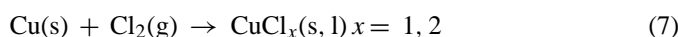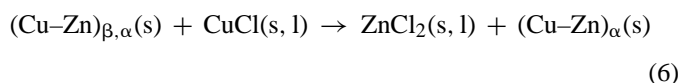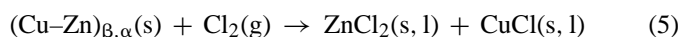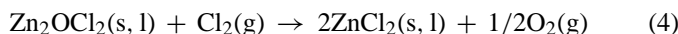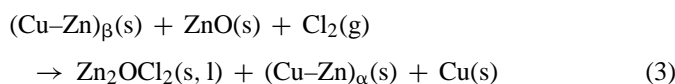

Fig. 8. (a) and (b) XRD pattern of the copper chlorides-Cu–Zn alloy mixture after 5 and 30 h, respectively. (c) and (d) SEM photograph of the copper chlorides-Cu–Zn alloy mixture after 5 and 30 h, respectively.
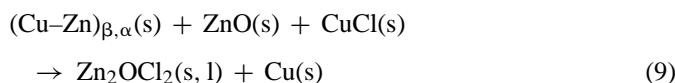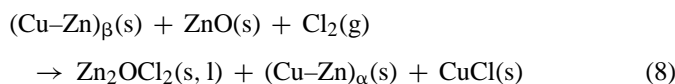
5. Discussion

Taking into account the results, the following reaction mechanism for the alloy chlorination is suggested:

$$(Cu\text{–}Zn)_\beta(s) + ZnO(s) + Cl_2(g)$$
$$\rightarrow Zn_2OCl_2(s, l) + (Cu\text{–}Zn)_\alpha(s) + Cu(s) \tag{3}$$

$$Zn_2OCl_2(s, l) + Cl_2(g) \rightarrow 2ZnCl_2(s, l) + 1/2O_2(g) \tag{4}$$

$$(Cu\text{–}Zn)_{\beta,\alpha}(s) + Cl_2(g) \rightarrow ZnCl_2(s, l) + CuCl(s, l) \tag{5}$$

$$(Cu\text{–}Zn)_{\beta,\alpha}(s) + CuCl(s, l) \rightarrow ZnCl_2(s, l) + (Cu\text{–}Zn)_\alpha(s) \tag{6}$$

$$Cu(s) + Cl_2(g) \rightarrow CuCl_x(s, l) \; x = 1, 2 \tag{7}$$

$(Cu\text{–}Zn)_\alpha(s)$ and $(Cu\text{–}Zn)_\beta(s)$ correspond to alpha and beta phases of the Cu–Zn alloy. The range of composition of these phases is Cu–(0–39)Zn (wt.%) and Cu–(36.7–59.8)Zn (wt.%), respectively [23].

The chlorination reaction starts at 250 °C with formation of zinc oxychloride from the thin layer of zinc oxide that covers the alloy surface and zinc from the alloy. The occurrence of α-Cu–Zn and metallic copper can be due to zinc preferential elimination from the alloy. However, metallic copper can also arise from the reaction of CuCl formed initially according to:

$$(Cu\text{–}Zn)_\beta(s) + ZnO(s) + Cl_2(g)$$
$$\rightarrow Zn_2OCl_2(s, l) + (Cu\text{–}Zn)_\alpha(s) + CuCl(s) \tag{8}$$

$$(Cu\text{–}Zn)_{\beta,\alpha}(s) + ZnO(s) + CuCl(s)$$
$$\rightarrow Zn_2OCl_2(s, l) + Cu(s) \tag{9}$$

All three species on the right hand side of Eq. (5) were detected by XRD in the chlorinated sample at 250 °C. CuCl as an intermediate specie according to Eqs. (8) and (9) has not been detected up to now. At 250 °C, the scale of oxichloride stops the reaction. At higher temperatures, due to the high reactivity of copper [7] great amounts of CuCl are quickly generated, which in turn reacts with zinc from the alloy inhibiting the protective effect of zinc oxichloride. Moreover, at high temperatures the chlorination of Zn_2OCl_2 is kinetically feasible. Both events inhibit the protective effect of the zinc oxichloride layer.

6. Conclusions

Differences in the alloy and pure metal reactivity were determined. Interactions were detected corresponding to oxidation–reduction reactions between copper chlorides and metallic zinc from the alloy. Mass gains show that volatilization of $ZnCl_2$ is diminished during alloy chlorination compared with chlorination of pure zinc.

Formation of well-developed copper crystals was observed.

At low temperatures the formation of a Zn_2OCl_2 layer inhibits the alloy chlorination reaction.

A global mechanism was presented according to the different processes considered: reaction inhibition, interactions between chlorides and copper crystallization.

References

[1] N. Bourhila, N. Thomas, J. Palleau, J. Torres, C. Bernard, R. Madar, Appl. Surf. Sci. 91 (1995) 175–181.
[2] I. Gaballah, M. Djona, J.C. Mugica, R. Solozabal, Resour. Conserv. Recycling 10 (1–2) (1994) 87–96.
[3] H. Wayne Richardson, Ullman's Encyclopedia of Industrial Chemistry, sixth ed., Electronic Release. Copper Compounds—Salts and Basic Salts, 2002.
[4] R. Tití -Manyaka, I. Iwasaki, Trans. SME/AIME 260 (1976) 282–288.
[5] W. Sesselmann, T.J. Chuang, Surf. Sci. 176 (1986) 32–66.
[6] W. Sesselmann, T.J. Chuang, Surf. Sci. 176 (1986) 67–90.
[7] G. De Micco, A.E. Bohé, D.M. Pasquevich, J. Alloys Compd. 437 (2007) 351–359.
[8] R. Tití-Manyaka, I. Iwasaki, SME Trans. 252 (1972) 307–313.
[9] J.P. Remeika, B. Batlogg, Mater. Res. Bull. 15 (1980) 1179–1182.
[10] L.S. Belknap, Aluminum Trichloride Production US Pat. 3,721,731, Cabot Corporation, Boston, Massachusetts, USA, 1973.
[11] R.E. Siemens, B.W. Jong, J.H. Russell, Conserv. Recycling 9 (2) (1986) 189–196.
[12] K. Matsumaru, M. Susa, K. Nagata, J. Iron Steel Inst. Jpn. 82 (10) (1996) 1–6.
[13] A. Landsberg, J. Less-Common Met. 159 (1990) 163–172.
[14] Y.N. Chang, F.I. Wei, J. Mater. Sci. 26 (1991) 3693–3698.
[15] G. De Micco, D.M. Pasquevich, A.E. Bohé, Thermochim. Acta 457 (2007) 83–91.
[16] J.A. González, F.C. Gennari, M. del Carmen Ruiz, A.E. Bohé, D.M. Pasquevich, Trans. Inst. Min. Met. Sect. C 107 (1998) 130–138.
[17] J.A. Chaudhary, J.D. Donaldson, S.M. Grimes, Heavy-metals in the environment. 5. The use of high copper–zinc residues in the zinc-chloride process and the recovery of copper as anhydrous copper(II) chloride, J. Chem. Tech. Biotechnol. 61 (1994) 293–297.
[18] D. Ferry, Y. Castrillejo, G. Picard, Electrochim. Acta 33 (1988) 1661.
[19] D. Ferry, Y. Castrillejo, G. Picard, Electrochim. Acta 34 (1989) 313.
[20] Y. Castrillejo, M.A. García, E. Barrado, P. Pasquier, G. Picard, Electrochim. Acta 40 (1995) 2731.
[21] Y. Castrillejo, A.M. Martinez, M. Vega, E. Barrado, G. Picard, J. Electroanal. Chem. 397 (1995) 139.
[22] M. Garcia, Y. Castrillejo, P. Pasquier, G. Picard, Molten Salt Forum 1–2 (1993–1994) 47.
[23] P. Villars, Pearson's Handbook of Crystallographica Data for Intermetallic Phases, Materials Park, ASM, 1991, p. 3027.
[24] A. Roine, Outokumpu HSC chemistry for Windows, 93001-ORGT version 2.0 Outokumpu Research Oy Information Service, 1994.
[25] D.L. Hildenbranda, K.H. Lau, Thermochemistry of ZnCl(g), J. Chem. Phys. 111 (3 (July)) (1999).
[26] D.R. Lide (Ed.), CRC Handbook of Chemistry and Physics, 85th ed., 2004–2005, CRC Press, pp. 4–95.

[27] A.E. Bohé, J.J. Andrade Gamboa, E.M. Lopasso, D.M. Pasquevich, Zirconium recovery from zircaloy shavings, J. Mater. Sci. 31 (1996) 3469–3474.

[28] J.R. Galvele, G.S. Duffó, Degradación de materiales corrosión, Monografía tecnológica nro. 3., UNSAM, CNEA, Instituto Sabato, Buenos Aires, 2006.

[29] G. De Micco, G.G. Fouga, A.E. Bohé, Chlorination of zinc oxide between 723 and 973 K, Metall. Mater. Trans. B 38 (6) (2007) 853–862.

[30] Joint Committee for Powder Diffraction Standards, International Center for Diffraction Data, Powder Diffraction File, 2001.